MnO2@Co3O4 nanocomposite based electrocatalyst for effective oxygen evolution reaction

Muhammad Yameen Solangi[1], Abdul Hanan Samo[2], Abdul Jaleel Laghari[1], Umair Aftab[1], Rehan Ali Qureshi[1], Muhammad Ishaque Abro[1] Muhammad Imran Irfan[3]

Abstract:

For large-scale energy applications, conceiving low-cost and simple earth-abundant electrocatalysts are more difficult to develop. By using an aqueous chemical technique, MnO2 was added into Co3O4 with varying concentrations to prepare MnO2@Co3O4 nanocomposite (CM). In an aqueous solution of 1 M KOH, the electrocatalyst with a greater concentration of MnO2 outperforms in terms of OER. To confirm the composition, crystalline structure, and morphology of the electrocatalyst, analytical methods such as X-ray diffraction (XRD) techniques, Fourier transformed infrared spectroscopy (FTIR) and scanning electron microscopy (SEM) were used. At 20 mA/cm2 current density, the electrocatalyst had a lowest overpotential of 310 mV verses Reversible hydrogen electrode (RHE). The CM-0.4 electrocatalyst has a small Tafel slope value and charge transfer resistance of approximately 72 mV/dec and 74 Ω which confirm its high catalytic activity. The electrocatalyst reveals a double layer capacitance (Rct) of 18 µF/cm2 and an electrochemical active surface area (ECSA) of 450 cm2, demonstrating that addition of MnO2 impurities into Co3O4 enhances the active catalyst sites. These findings contribute to the knowledge of these kind of catalysts, that will assist in the development of novel electrocatalysts which are feasible for prospective energy generation technologies.

Keywords: *Electrocatalyst; oxygen evolution reaction; cobalt oxide; manganese oxide; alkaline media.*

1. Introduction

Growing energy consumption and the depletion of fossil fuels are two major challenges which have led to the discovery of earth abundant alternative sources and the development of effective energy storage systems [1-3]. For this fact, electrochemical water electrolysis is one of the most efficient methods to obtain hydrogen [4,5].

Herein, hydrogen evolution reaction (HER) takes place at the cathode while oxygen evolution reaction (OER) happens at the anode in an electrochemical water splitting mechanism. Nevertheless, the efficient electrocatalysts were utilized for effective water splitting [6-8]. Currently, the RuO2/IrO2 based noble electrocatalysts have superiority for OER with lower low overpotential value for higher electro-catalytical activity [9,10].

However, they are rare in nature and massive cost electrocatalyst that restrict the usage in industrial applications. To achieve cost-effective hydrogen generation, creating an electro-catalyst for water splitting that are

[1]Dept. of Metallurgy & Materials Engineering, MUET, Jamshoro, Pakistan.
[2]College of Materials & Chemical Engineering, Harbin Engineering University, Harbin, China.
[3]Institute of Chemistry, University of Sargodha, Sargodha- 40100 Pakistan
Corresponding Author: yameen.engineer14@gmail.com

efficient, inexpensive, earth-abundant, stable, and operate at low overpotential is critical [11-13].

The OER mechanism contains 4 electron charge transfer kinetics [14]. Therefore, OER mechanism is slow process as compared to HER and responsible for overall performance of water splitting. In this regard, OER requires more overpotential for water oxidation which provide the major hindrance in water splitting technology [15-17]. So that, researchers are developing electrocatalysts for OER with low overpotential, ease of synthesis and low-cost. In this fact, various transition metal oxides, sulfides, selenides, and phosphide based electrocatalysts were developed to overcome such problems [18-20].

In this work, the impurity addition strategy was applied to create nanocomposite for essential OER performance. Wherein, MnO_2 as an impurity was added in Co_3O_4 to create oxygen vacancies in the Co_3O_4 nanostructures which may be responsible for increase in active sites and decrease the overpotential of catalyst that leads to superior OER performance. The synthesized nanocomposite was characterized by XRD, FTIR, SEM and Electrochemical Analysis for the determination of crystallinity, phase purity, morphology, and electrochemical investigation respectively.

2. Experimental Work

2.1 Materials and Methods

Cobalt chloride hexahydrate ($CoCl_2.6.H_2O$), urea (CH_4N_2O) and potassium permanganate ($KMnO_4$) were brought from Sigma Aldrich, Karachi, Pakistan. The synthesis of $MnO_2@Co_3O_4$ nanocomposite was developed by aqueous chemical method [21]. Herein, 0.1M solution of $CoCl_2.6.H_2O$ and CH_4N_2O was added into 100 ml deionized water. After that, $KMnO_4$ with two different concentrations i.e., 0.2 g and 0.4 g were added separately in different breakers containing cobalt oxide precursor. These samples were labeled as Co_3O_4 pristine, CM-0.2 and CM-0.4. The label CM denotes the composite of $MnO_2@Co_3O_4$.

These samples were mixed properly and placed into an electric oven at 95OC for 5 h. Once the reaction time was completed then samples were taken out from oven and washed multiple times with deionized (DI) water to remove the extra impurities. After that, nanocomposite material was collected through sedimentation method in china dish and dried in oven at 100OC for moisture content removal. The dried samples were placed into furnace for calcination to convert hydroxide phase into oxide phase at 500OC for 5 h. When the calcination time finished then sample were taken from furnace and nanocomposite was achieved for further characterization.

2.2 Physical Characterization

Powder X-ray diffraction (XRD) was performed on a Philips PAN analytical powder x-ray diffractometer at 45 kV and 45 mA using Cu Kα radiation (λ = 0.15406 nm). The lattice parameters were calculated by Bragg's law in cubic formula.

$$d_{(hkl)} = \frac{a}{\sqrt{h^2 + k^2 + l^2}}$$

Whereas, "d(hkl)" is the atomic planer spacing, "a" is lattice constant and "(h,k,l)" is the diffracted plane.

The Crystallite size of sample was computed by Debye's Scherrer equation at (311) plane.

$$D = \frac{k\lambda}{\beta Cos\theta}$$

where "D" is the crystallite size (Å), "k" is Scherrer constant that is equal to 0.9, "λ" is the wavelength of source CuKα, "β" is the full width at half maximum (Radians) and "θ" is the peak position (Radians).

Fourier transform infrared spectroscopy (FTIR) was obtained on a Perkin Elmer FTIR Spectrometer spectrum two. Scanning electron microscopy (SEM) images were achieved on JSM-6380L JEOL scanning electron microscope.

2.3 Electrochemical Analysis

Electrochemical measurements were carried out on a VERSASTAT 4-500 Potentiostat consisting of a three-electrode assembly i.e., working electrode, reference

electrode and counter electrode made up of glassy carbon electrode, silver-silver chloride electrode and Pt wire respectively. Glassy carbon electrodes were modified with the electrocatalyst, and various experiments were performed in 1M KOH solution. The linear sweep voltammetry (LSV) was done to determine the polarization curves at a scan rate of 5 mV/s and cyclic voltammetry (CV) was used to investigate the effective active surface area at 10, 20 and 30 mV/s scan rates. The chrono-potentiometric analysis was accomplished for durability as synthesized electrocatalyst at 20 mA/cm2 for 40 h.

3. Results and Discussion

3.1 Physical Characterization

The XRD spectrum of pristine Co3O4, CM-0.2 and CM-0.4 can be seen in Fig.1. The XRD spectra of pristine Co3O4 resembled with JCPDS card no. 01-080-1536. The diffraction pattern revealed at the planes of (111), (220), (311), (222), (400), (331), (422), (511), (440), (531), (442), (620), (533) and (622) at the 2 theta angles of 18.848o, 31.017o, 36.461o, 38.231o, 44.436o, 48.669o, 55.177o, 58.842o, 64.656o, 68.011o, 69.111o, 73.437o, 76.618o and 77.668o respectively. This JCPDS card validates that the Co3O4 has cubic crystalline structure [22,23]. Whereas XRD spectrum of MnO2 are matched with JCPDS card no. 00-044-0992 that diffracted at 2θ values of 19.112o, 37.121o, 38.958o, 45.068o, 49.498o, 59.599o, 65.703o and 69.583o corresponded at the planes (111), (311), (222), (400), (331), (511), (531) and (440). which revealed that MnO2 is also in cubic crystalline phase.

In addition, other structural features such atomic planer spacing, lattice constant and crystallite size of samples are given in the Table 1. The lattice constant of pristine Co3O4 is higher but the addition of MnO2 reduces its lattice constant that leads to reduction in crystallite size. Here, the substitution of large Co2+ atom (0.72 Å) with small Mn4+ atom (0.67 Å) carried out that may be responsible for shrinkage of unit cell and achieved reduction in the lattice constant. However, the major peak of Co3O4 at (311) diffracted plane

shifted toward right side as the concentration of MnO2 increases as shown in Fig 1(b) which also suggested the substitution of Co atom by Mn atom. Therefore, crystallite size of composite decreases as the concentration of MnO2 increases [24,25].
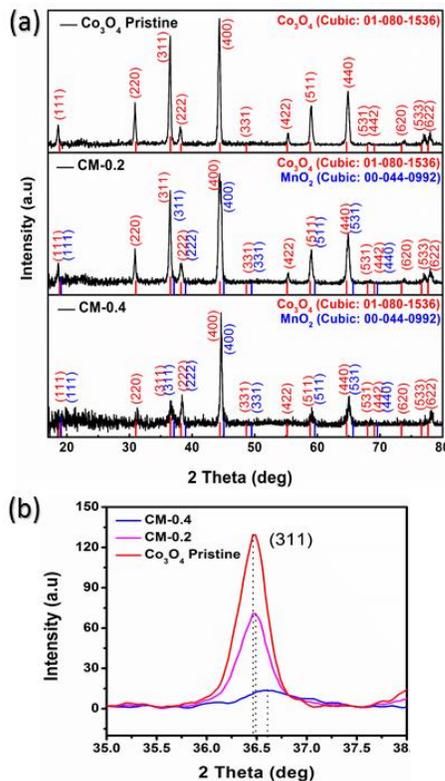
Fig. 1. (a) XRD pattern of various samples (b) Zoom in view of XRD peak shift

The FTIR spectra of various samples are shown in Fig. 2. It represented that pristine Co3O4, CM-0.2 and CM-0.4 involved same peak of O-H, C-H, C=O, O-H, C-O and C=C corresponding to 3438 cm-1, 2927cm-1, 1797cm-1, 1035 cm-1 and 878 cm-1. These organic bonds achieved from the Potassium bromide (KBr) that were used for the making the pallet of KBr and sample for FTIR measurement. Despite this, the main difference was observed in pristine Co3O4 and nanocomposite (CM-0.4) of metal oxide M-O peaks which represent O-Co-O at 570 cm-1 and Co-O at 663 cm-1. However, the presence

of MnO2 in Co3O4 nanostructures sharpen the metal oxide peaks due to the addition of MnO2 impurities [22,26,27].
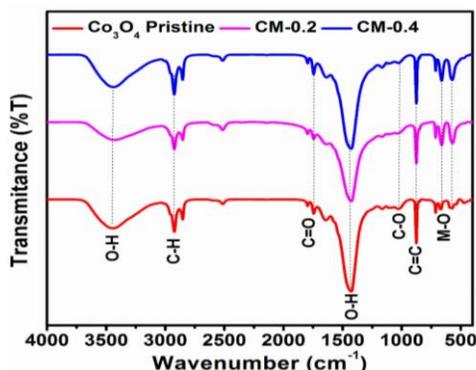
Fig. 2. FTIR spectra of different samples
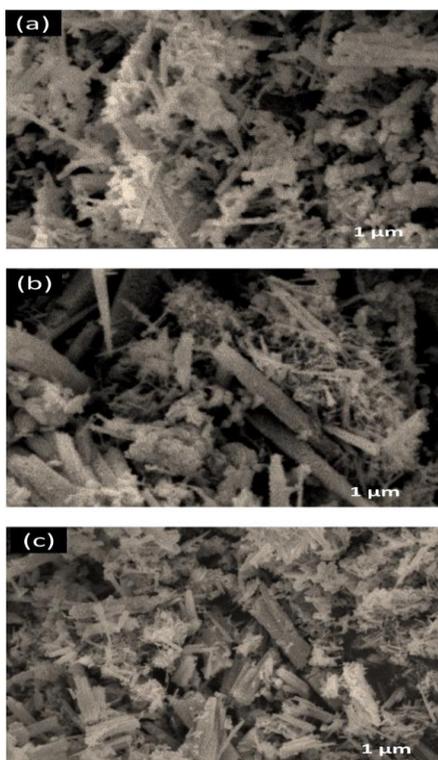
Fig. 3. SEM images of (a) Pristine Co_3O_4 (b) CM-0.2 (c) CM-0.4

The morphology of prepared Co3O4 pristine and nanocomposites was examined by scanning electron microscopy (SEM). The SEM images of samples are shown in Fig. 3. The morphology of pristine Co3O4 showed nano needles like structure as shown in Fig. 3(a) while the morphology of CM-0.2 and CM-0.4 contained nano flakes in the matrix of nano needles like structure as shown in Fig. 3(b, c). It can be seen that CM-0.2 nanocomposite contained fewer nano flakes than CM-0.4. which stated that as the amount of MnO2 increase then nano flakes concentration increases in nano needle matrix.

3.2 Electrochemical Analysis

The electrochemical analysis of various samples was investigated in 1M KOH environment. The LSV polarization curves can be seen in Fig. 4(a) that shows CM-0.4 has lowest overpotential of 310 mV as compare to the overpotential of pristine Co3O4 and CM-0.2 as 430 mV and 350 mV vs RHE at the current density of 20 mA/cm2. The CM-0.4 electrocatalyst exhibits high OER performance due to lowest overpotential as compare to updated electrocatalyst that can be seen in Table 3. The Tafel values were obtained by linear fit region of polarization curves as shown in Fig. 4(b). The Tafel values of pristine Co3O4, CM-0.2 and CM-0.4 are calculated as 102 mV/dec, 86 mV/dec and 72 mV/dec respectively.

The oxygen evolution reaction (OER) takes place through four electron transfer mechanism which is given as under.

1. $M + OH^- \rightarrow MOH + e^-$
2. $MOH + OH^- \rightarrow MO^- + H_2O$
3. $MO^- \rightarrow MO + e^-$
4. $2MO \rightarrow 2M + O_2 + 2e-$

The OER kinetic and theoretical Tafel values in alkaline media of 1, 2, 3 and 4 sub reactions are 120 mV/dec, 60 mV/dec, 40 mV/dec and 15 mV/dec respectively [28, 29]. Therefore, the current study contains 72 mV/dec Tafel value of best composite which suggest that step-1 is rate determining step for effective OER performance.
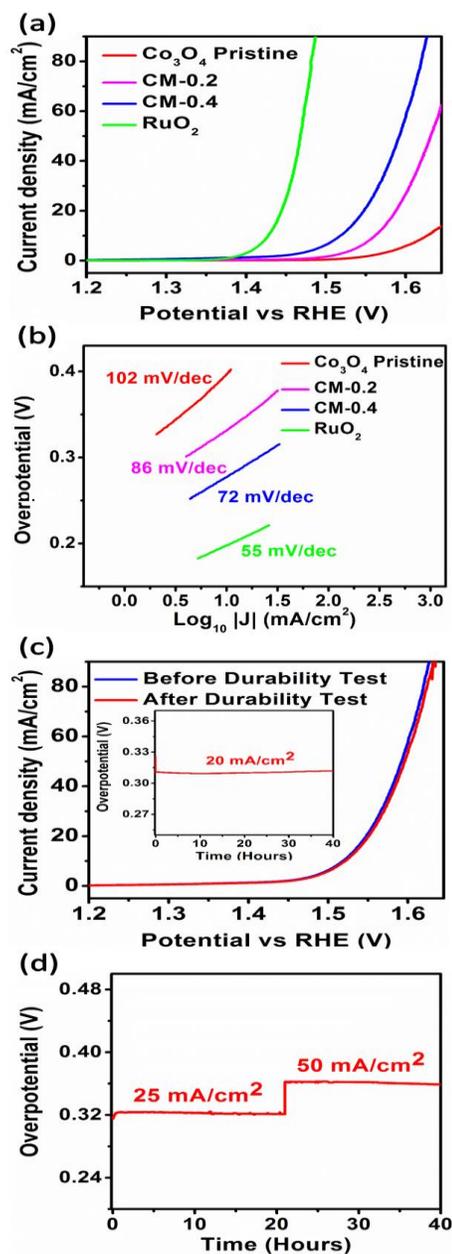
Fig. 4. Electrochemical Analysis of various electrocatalysts (a) Polarization curve (b) Tafel plot (c) Stability & Durability of best sample (d) Durability of best electrocatalyst at different current densities.

The stability test was performed by measuring LSV before and after chronopotentiometry at 20 mA/cm2. The stability of CM-0.4 illustrated in Fig. 4(c) which represented its overpotential did not drop after long operation. Furthermore, the durability of CM-0.4 can be seen inside Fig. 4(c) which showed that CM-0.4 electrocatalyst is long term durable for 40 h. In addition, durability test was also performed at different current densities i.e., 25 mA/cm2 and 50 mA/cm2 as shown in Fig. 4(d). It revealed that the potential does not drop at various current densities which give significant proof of electrocatalyst's stability.

The cyclic voltammetric (CV) experiment was performed at different scan rates on various electrocatalysts as shown in Fig. 5. The cyclic voltammetry of CM-0.4 has highest current density that represent its highest catalytical active sites as seen in Fig. 5(c). In addition, the double layer capacitance Cdl value plots were extracted from CV curves as illustrated in Fig. 5(d). The Cdl values of pristine Co3O4, CM-0.2 and CM-0.2 have been calculated as 3.6 µF/cm2, 7.8 µF/cm2 and 18 µF/cm2. The CM-0.4 electrocatalyst has high double layer capacitance than other as prepared electrocatalysts.

The electrochemical active surface area ESCA was calculated by Cdl/Cs expression, whereas specific capacitance of the electrolyte (Cs) in 1M KOH is about 0.04 [30]. The electrochemical active surface area (ECSA) was calculated as 450 cm2, 195 cm2, and 90 cm2 for CM-0.4, CM-0.2 and Pristine Co3O4 respectively which are mentioned in Table 2. This data also authenticates the catalytical performance of CM-0.4.

The electrochemical impedance spectroscopy data represented by Nyquist plot and Bode (1, 2) of various samples are shown in Fig. 6. The EIS data was fitted via Z view software and fitted equivalent circuit is enclosed in Fig. 6(a). The solution resistance Rs is almost similar to all samples due to similar electrolyte conditions. The charge transfer resistance Rct was obtained as 74 Ω, 240 Ω and 460 Ω of CM-0.4, CM-0.2 and pristine Co3O4 respectively. The results also

validate that the Rct of nanocomposite based electrocatalyst is lower than pristine electrocatalyst which facilitates the movement of charge in between anode and cathode via electrolyte.

The bode-1 plot gives the information about gain parameter and phase angle in the range of 0.1Hz to 100kHz frequency at 1.45V applied potential. The phase angles obtained as pristine Co3O4 (50.123o), CM-0.2 (45.537o) and CM-0.4 (31.289o) that confirm the superior activity of CM-0.4 electrocatalyst. Furthermore, the bode-2 plot provides the knowledge about maximum oscillation frequency of catalyst. It was noticed that CM-0.4 contained least oscillation frequency as compared to other two catalyst. Therefore, better adsorption of reactive species on the surface of electrocatalysts is attributed due to greater electron recombination lifetime. From these outcomes, it is suggested that CM-0.4 electrocatalyst can be potential candidate for superior water oxidation reaction.

Fig. 5. Cyclic voltammetry of various electrocatalysts (a) Pristine Co_3O_4 (b) CM-0.2 (c) CM-0.4 (d) Double layer capacitance (C_{dl}) plot.
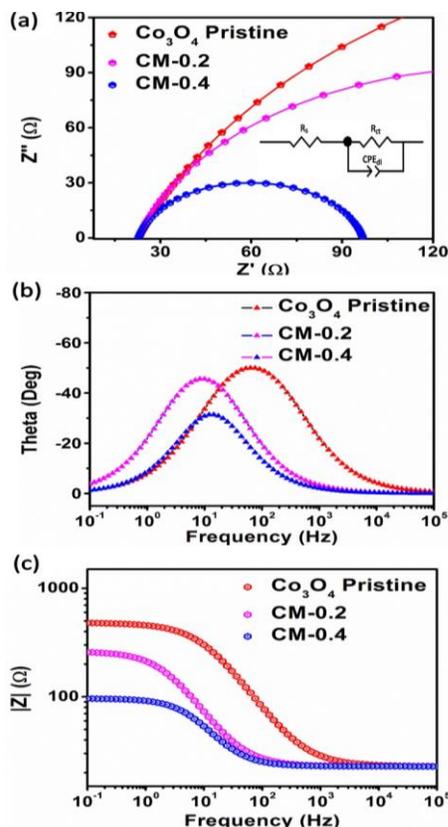
Fig. 6. Electrochemical impedance spectroscopy data of pristine Co_3O_4, CM-0.2 and CM-0.4 (a) Nyquist plot (b) Bode plot-1 and (c) Bode plot-2

TABLE I.   XRD STRUCTURAL FEATURES OF PRISTINE AND COMPOSITE SAMPLES.

Sample IDs	(hkl)	2 Theta	d spacing	Lattice Constant	FWHM	Crystallite Size (D)
		Degree	Å	Å	Degree	Å
Co_3O_4 Pristine	(311)	36.4617	2.4622	8.4118	0.28356	294.96
CM-0.2	(311)	36.470	2.4617	8.4051	0.30115	277.74
CM-0.4	(311)	36.658	2.4495	8.3821	0.60382	138.59

TABLE II.   SUMMARY OF UNIQUE FEATURES OF PRESENTED OER CATALYSTS

Catalyst	Calculated from LSV	Calculated from EIS		Calculated from CV	
	Tafel Slope	Charge Transfer Resistance	Double Layer Capacitance	Double Layer Capacitance	Electrochemically active surface area
	B	R_{ct}	CPE_{dl}	C_{dl}	$ECSA$
	mV/dec	Ω	Mf	$(\mu F/cm^2)$	cm^2
Co_3O_4 Pristine	102	460	0.04	3.6	90
CM-0.2	86	240	0.31	7.8	195
CM-0.4	72	74	0.37	18	450

TABLE III.   COMPARISON OF CM-0.4 COMPOSITE AS OER CATALYST WITH RECENTLY REPORTED ELECTROCATALYSTS.

Electrocatalyst	Electrolyte	Current Density	Overpotential	References
$MnO_2@Co_3O_4$ (CM-0.4)	1 M KOH	20 mA/cm^2	310 mV	This work
Mg/Co_3O_4	1 M KOH	20 mA/cm^2	320 mV	[31]
Fe_3O_4/Co_3O_4	1 M KOH	10 mA/cm^2	370 mV	[13]
$CoSe_4$	1 M KOH	10 mA/cm^2	320 mV	[32]
Mn-Co Phosphide	1 M KOH	10 mA/cm^2	330 mV	[33]
$NiCo_2S_4/RGO$	1 M KOH	10 mA/cm^2	366 mV	[34]
$CoOx-N-C/TiO_2C$	1 M KOH	10 mA/cm^2	350 mV	[35]

4. Conclusion

The summery of present work involves the MnO2@Co3O4 nanocomposite based electrocatalysts which have been synthesized by aqueous chemical method. The XRD pattern and FTIR spectrum validate the synthesis of pristine Co3O4 and CM-nanocomposite. The CM-0.4 catalyst having morphology of nano flakes in the matrix of nano needles exhibits lowest overpotential of 310 mV at current density of 20 mA/cm2. It also contains low Tafel slope value and Rct value as 72 mv/dec and 74 Ω respectively. This electrocatalyst has expressed higher ECSA of 450 cm2. In addition, it is stable and long-term durable for 40 h that makes it superior for OER activity.

DATA AVAILABILITY STATEMENT

It is stated that this data is soul property of authors and not taken from any data base. The authors also declare that this data is not published in any other journal.

AUTHOR CONTRIBUTION

All authors equally contribute for this work

CONFLICT OF INTEREST

The authors declare no conflict of interest.

ACKNOWLEDGMENT

REFERENCES

[1] U. Aftab, A. Tahira, R. Mazzaro, M. I. Abro, M. M. Baloch, M. Willander, et al., "The chemically reduced CuO–Co3O4 composite as a highly efficient electrocatalyst for oxygen evolution reaction in alkaline media," Catalysis Science & Technology, vol. 9, pp. 6274-6284, 2019.

[2] A. Mehboob, S. R. Gilani, A. Anwar, A. Sadiqa, S. Akbar, and J. Patujo, "Nanoscale cobalt-oxide electrocatalyst for efficient oxygen evolution reactions in alkaline electrolyte," Journal of Applied Electrochemistry, vol. 51, pp. 691-702, 2021.

[3] P. F. Liu, H. Yin, H. Q. Fu, M. Y. Zu, H. G. Yang, and H. Zhao, "Activation strategies of water-splitting electrocatalysts," Journal of Materials Chemistry A, vol. 8, pp. 10096-10129, 2020.

[4] A. Tahira, U. Aftab, M. Y. Solangi, A. Gradone, V. Morandi, S. S. Medany, et al., "Facile deposition of palladium oxide (PdO) nanoparticles on CoNi2S4 microstructures towards enhanced oxygen evolution reaction," Nanotechnology, 2022.

[5] Z. H. Ibupoto, A. Tahira, A. A. Shah, U. Aftab, M. Y. Solangi, J. A. Leghari, et al., "NiCo2O4 nanostructures loaded onto pencil graphite rod: An advanced composite material for oxygen evolution reaction," International Journal of Hydrogen Energy, vol. 47, pp. 6650-6665, 2022.

[6] A. Q. Mugheri, A. Tahira, U. Aftab, A. L. Bhatti, R. Lal, M. A. Bhatti, et al., "Chemically Coupled Cobalt Oxide Nanosheets Decorated onto the Surface of Multiwall Carbon Nanotubes for Favorable Oxygen Evolution Reaction," Journal of Nanoscience and Nanotechnology, vol. 21, pp. 2660-2667, 2021.

[7] B. Paul, P. Bhanja, S. Sharma, Y. Yamauchi, Z. A. Alothman, Z.-L. Wang, et al., "Morphologically controlled cobalt oxide nanoparticles for efficient oxygen evolution reaction," Journal of Colloid and Interface Science, vol. 582, pp. 322-332, 2021.

[8] C. L. I. Flores and M. D. L. Balela, "Electrocatalytic oxygen evolution reaction of hierarchical micro/nanostructured mixed transition cobalt oxide in alkaline medium," Journal of Solid State Electrochemistry, vol. 24, pp. 891-904, 2020.

[9] W. H. L. P. D. Jaekyung Yia, Chang Hyuck Choi (Ph.D.), Yuri Lee (Ph.D.), Kyung Su Park (Ph.D.), Byoung Koun Min (Ph.D.), Yun Jeong Hwang (Ph.D.), Hyung-Suk Oh (Ph.D., "Effect of Pt introduced on Ru-based electrocatalyst for oxygen evolution activity and stability," Electrochemistry Communications, vol. 104, p. 106469, 2019.

[10] Q. Shi, C. Zhu, D. Du, and Y. Lin, "Robust noble metal-based electrocatalysts for oxygen evolution reaction," Chem Soc Rev, vol. 48, pp. 3181-3192, 2019.

[11] D. Zhao, Z. Zhuang, X. Cao, C. Zhang, Q. Peng, C. Chen, et al., "Atomic site electrocatalysts for water splitting, oxygen reduction and selective oxidation," Chemical Society Reviews, vol. 49, pp. 2215-2264, 2020.

[12] A. Tahira, Electrochemical water splitting based on metal oxide composite nanostructures vol. 2066. Linköping: Linköping University Electronic Press, 2020.

[13] A. L. Bhatti, U. Aftab, A. Tahira, M. I. Abro, R. H. Mari, M. K. Samoon, et al., "An Efficient and Functional Fe3O4/Co3O4 Composite for Oxygen Evolution Reaction," Journal of Nanoscience and Nanotechnology, vol. 21, pp. 2675-2680, 2021.

[14] A. Hanan, A. J. Laghari, M. Y. Solangi, U. Aftab, M. I. Abro, D. Cao, et al., "CdO/Co3O4

Nanocomposite as an Efficient Electrocatalyst for Oxygen Evolution Reaction in Alkaline Media," International Journal of Engineering Science Technologies, vol. 6, pp. 1-10, 2022.

[15] Y. V. Kaneti, Y. Guo, N. L. W. Septiani, M. Iqbal, X. Jiang, T. Takei, et al., "Self-templated fabrication of hierarchical hollow manganese-cobalt phosphide yolk-shell spheres for enhanced oxygen evolution reaction," Chemical Engineering Journal, vol. 405, p. 126580, 2021.

[16] I. M. Abdullahi, J. Masud, P.-C. Ioannou, E. Ferentinos, P. Kyritsis, and M. Nath, "A Molecular Tetrahedral Cobalt–Seleno-Based Complex as an Efficient Electrocatalyst for Water Splitting," Molecules, vol. 26, p. 945, 2021.

[17] A. L. Bhatti, U. Aftab, A. Tahira, M. I. Abro, M. Kashif samoon, M. H. Aghem, et al., "Facile doping of nickel into Co3O4 nanostructures to make them efficient for catalyzing the oxygen evolution reaction," RSC Advances, vol. 10, pp. 12962-12969, 2020.

[18] C. Linder, S. G. Rao, A. le Febvrier, G. Greczynski, R. Sjövall, S. Munktell, et al., "Cobalt thin films as water-recombination electrocatalysts," Surface and Coatings Technology, vol. 404, p. 126643, 2020.

[19] A. Badreldin, A. E. Abusrafa, Abdel, and A. Wahab, "Oxygen-Deficient Cobalt-Based Oxides for Electrocatalytic Water Splitting," ChemSusChem, vol. 14, pp. 10-32, 2021.

[20] A. Badruzzaman, A. Yuda, A. Ashok, and A. Kumar, "Recent advances in cobalt based heterogeneous catalysts for oxygen evolution reaction," Inorganica Chimica Acta, vol. 511, p. 119854, 2020.

[21] M. R. S. A. Janjua, "Synthesis of Co3O4 Nano Aggregates by Co-precipitation Method and its Catalytic and Fuel Additive Applications," Open Chemistry, vol. 17, pp. 865-873, 2019.

[22] D. D. M. Prabaharan, K. Sadaiyandi, M. Mahendran, and S. Sagadevan, "Precipitation method and characterization of cobalt oxide nanoparticles," Applied Physics A, vol. 123, 2017.

[23] M. Y. Solangi, U. Aftab, A. Tahira, M. I. Abro, R. Mazarro, V. Morandi, et al., "An efficient palladium oxide nanoparticles@Co3O4 nanocomposite with low chemisorbed species for enhanced oxygen evolution reaction," International Journal of Hydrogen Energy, vol. 47, pp. 3834-3845, 2022.

[24] L. Abdelhak, B. Amar, B. Bedhiaf, D. Cherifa, and B. Hadj, "Characterization of Mn-Doped Co3O4 Thin Films Prepared by Sol Gel-Based Dip-Coating Process," High Temperature Materials and Processes, vol. 38, pp. 237-247, 2019.

[25] N. Manjula, M. Pugalenthi, V. S. Nagarethinam, K. Usharani, and A. R. Balu, "Effect of doping concentration on the structural, morphological, optical and electrical properties of Mn-doped CdO thin films," Materials Science-Poland, vol. 33, pp. 774-781, 2015.

[26] T. Athar, A. Hakeem, N. Topnani, and A. Hashmi, "Wet Synthesis of Monodisperse Cobalt Oxide Nanoparticles," ISRN Materials Science, vol. 2012, pp. 1-5, 2012.

[27] A. N. Naveen and S. Selladurai, "Investigation on physiochemical properties of Mn substituted spinel cobalt oxide for supercapacitor applications," Electrochimica Acta, vol. 125, pp. 404-414, 2014.

[28] U. Aftab, A. Tahira, R. Mazzaro, V. Morandi, M. I. Abro, M. M. Baloch, et al., "Facile NiCo2S4/C nanocomposite: an efficient material for water oxidation," Tungsten, vol. 2, pp. 403-410, 2020.

[29] A. Q. Mugheri, A. Tahira, U. Aftab, M. I. Abro, A. B. Mallah, G. Z. Memon, et al., "An advanced and efficient Co3O4/C nanocomposite for the oxygen evolution reaction in alkaline media," RSC Advances, vol. 9, pp. 34136-34143, 2019.

[30] A. Tahira, Z. H. Ibupoto, M. Vagin, U. Aftab, M. I. Abro, M. Willander, et al., "An efficient bifunctional electrocatalyst based on a nickel iron layered double hydroxide functionalized Co3O4 core shell structure in alkaline media," Catalysis Science & Technology, vol. 9, pp. 2879-2887, 2019.

[31] A. H. Samo, U. Aftab, M. Yameen, A. J. Laghari, M. Ahmed, M. N. Lakhan, et al., "MAGNESIUM DOPED COBALT-OXIDE COMPOSITE FOR ACTIVE OXYGEN EVOLUTION REACTION," Journal of Applied and Emerging Sciences, vol. 02, pp. 210-216, 2021

[32] I. M. Abdullahi, J. Masud, P.-C. Ioannou, E. Ferentinos, P. Kyritsis, and M. Nath, "A Molecular Tetrahedral Cobalt–Seleno-Based Complex as an Efficient Electrocatalyst for Water Splitting," Molecules, vol. 26, p. 945, 2021.

[33] Y. V. Kaneti, Y. Guo, N. L. W. Septiani, M. Iqbal, X. Jiang, T. Takei, et al., "Self-templated fabrication of hierarchical hollow manganese-cobalt phosphide yolk-shell spheres for enhanced oxygen evolution reaction," Chemical Engineering Journal, vol. 405, p. 126580, 2021.

[34] C. Shuai, Z. Mo, X. Niu, X. Yang, G. Liu, J. Wang, et al., "Hierarchical NiCo2S4 nanosheets grown on graphene to catalyze the oxygen evolution reaction," Journal of Materials Science, vol. 55, pp. 1627-1636, 2020.

[35] L. He, J. Liu, B. Hu, Y. Liu, B. Cui, D. Peng, et al., "Cobalt oxide doped with titanium dioxide and embedded with carbon nanotubes and graphene-like nanosheets for efficient trifunctional electrocatalyst of hydrogen evolution, oxygen reduction, and oxygen evolution reaction," Journal of Power Sources, vol. 414, pp. 333-344, 2019.